*Acta Cryst.* (1999). B**55**, 78–84

# Experimental charge density and electrostatic potential in nicotinamide

Yoshihisa Miwa,[a] Takashi Mizuno,[a] Kazunori Tsuchida,[a] Tooru Taga[a]* and Yutaka Iwata[b]

[a]*Faculty of Pharmaceutical Sciences, Kyoto University, Sakyo-ku, Kyoto 606-11, Japan, and* [b]*Research Reactor Institute, Kyoto University, Kumatori, Sennan-gun, Osaka 590-04, Japan. E-mail: taga@pharm.kyoto-u.ac.jp*

(*Received 11 October 1997; accepted 3 June 1998*)

## Abstract

The accurate crystal structure of nicotinamide, 3-pyridinecarboxamide, was determined from X-ray and neutron diffraction experiments: $C_6H_6N_2O$, $M_r = 122.13$, monoclinic, $P2_1/c$, $Z = 4$. The electron distribution at 150 K was determined by the maximum entropy method and the electrostatic potential in the crystal was calculated by Fourier convolution of the electron distribution. The electrostatic properties of the nicotinamide molecule depend on the molecular conformation. The asymmetric electrostatic potential field observed above and below the pyridine-ring plane is related to the rotation of the carboxamide group with respect to the pyridine plane. The positive potential peak at the C4 atom of the pyridine ring extends to the C═O-group side of the plane. The asymmetry of the potential on the C4 atom is consistent with the stereospecificity of hydride transfer in $NAD^+$/NADH oxidoreduction.

## 1. Introduction

The crystal structure of nicotinamide was first determined by Wright & King (1954) and it has not been re-examined in any detail since. The nicotinamide ring is the reactive part of nicotinamide adenine dinucleotide (NAD) and its phosphate (NADP), which are the major electron carriers in many biological oxidation–reduction reactions. It is well known that the stereochemistry of NAD is controlled by a number of dehydrogenation enzymes (You *et al.*, 1978; Nambiar *et al.*, 1983). When the coenzyme has formed a reactive complex with an enzyme, the carboxamide group loses freedom of rotation owing to intermolecular binding forces such as hydrogen bonds. The characteristic reaction is the transfer of the hydride ion from the substrate to the 4 position of the nicotinamide moiety of $NAD^+$. Experimental and theoretical studies on the model compounds for the reaction have suggested that the favored reaction involves hydride transfer to the face of the pyridine ring near the carbonyl oxygen (de Kok *et al.*, 1986; Ohno *et al.*, 1986; Wu & Houk, 1991, 1993). Based on the quantum-chemical energy calculations of the transition state by Donkersloot & Buck (1981) it has been explained that the stereospecific property of the reaction is induced by the interaction between the negatively charged O atom of the carboxamide group and the positive charge of the hydride-donating moiety. Information on such a relationship between the electronic properties and molecular conformations of nicotinamide will enable the electron and hydride transfer reaction in the biological redox processes to be better understood.

The aim of the present research is the determination of an accurate crystal structure of nicotinamide and to obtain the detailed electron density distribution in a nicotinamide molecule. The electron distributions were calculated by the maximum entropy method, since this method has the merit that the distributions can be obtained without assuming the function forms of the atomic form factors and displacement factors for each atom. The electrostatic potential in the crystal was calculated by the Fourier-convolution method from the experimental charge densities.

## 2. Experimental

### 2.1. *X-ray data*

Nicotinamide was recrystallized from ethylene glycol–water solution by slow evaporation. A Rigaku AFC5-RU200 four-circle diffractometer equipped with a Rigaku MJ10224A cryostat apparatus was used. Two sets of X-ray reflection data, at 150 and 295 K, were collected. Intensities were measured by the $\omega/2\theta$-scan technique with an $\omega$-scan width of $(1.73 + 0.30\tan\theta)^\circ$ at the maximum scan speed of $4^\circ$ min$^{-1}$. The data were converted to $F$ values corrected for Lorentz–polarization factors but not for absorption. In the experiment at 150 K the data collection was performed in several separate series of measurements in order to supply liquid nitrogen to the equipment. The temperature was reset for each series in order to avoid frosting on the surface of the specimen and the orientation matrix was redetermined for each reset. The positional and anisotropic displacement parameters of the non-H atoms were refined by the full-matrix least-squares method. Further details are given in Table 1.

### 2.2. *Neutron study*

A single crystal was grown from ethylene glycol–water (4/6) solution for the neutron diffraction study. It was mounted on a four-circle neutron diffractometer

Table 1. *Experimental details*

| | 150 K (X-ray) | 295 K (X-ray) | 295 K (neutron) |
|---|---|---|---|
| Crystal data | | | |
| Chemical formula | $C_6H_6N_2O$ | $C_6H_6N_2O$ | $C_6H_6N_2O$ |
| Chemical formula weight | 122.13 | 122.13 | 122.13 |
| Cell setting | Monoclinic | Monoclinic | Monoclinic |
| Space group | $P2_1/c$ | $P2_1/c$ | $P2_1/c$ |
| $a$ (Å) | 3.877 (4) | 3.975 (5) | 3.975 (5) |
| $b$ (Å) | 15.60 (1) | 15.632 (8) | 15.632 (8) |
| $c$ (Å) | 9.375 (6) | 9.422 (4) | 9.422 (4) |
| $\beta$ (°) | 98.45 (7) | 99.03 (7) | 99.03 (7) |
| $V$ (Å$^3$) | 560.8 | 578.2 | 578.2 |
| $Z$ | 4 | 4 | 4 |
| $D_x$ (Mg m$^{-3}$) | 1.4463 | 1.4028 | 1.4028 |
| $D_m$ (Mg m$^{-3}$) | — | 1.398 | 1.398 |
| Density measured by | — | Flotation | Flotation |
| Radiation type | Mo $K\alpha$ | Mo $K\alpha$ | Neutron |
| Wavelength (Å) | 0.71073 | 0.71073 | 1.005 (3) |
| No. of reflections for cell parameters | 25 | 25 | — |
| $\theta$ range (°) | 8.41–13.46 | 8.14–13.46 | — |
| $\mu$ (mm$^{-1}$) | 0.103 | 0.1 | 0.827 |
| Temperature (K) | 150 | 295 | 295 |
| Crystal size (mm) | 0.7 × 0.7 × 0.6 | 0.8 × 0.7 × 0.6 | 6.0 × 4.0 × 4.0 |
| Crystal color | Colorless | Colorless | Colorless |
| Data collection | | | |
| Diffractometer | Rigaku AFC5-RU200 | Rigaku AFC5-RU200 | Four-circle |
| Data collection method | $\omega/2\theta$ scans | $\omega/2\theta$ scans | $\omega/2\theta$ scans |
| Absorption correction | None | None | None |
| No. of measured reflections | 6781 | 5771 | 1748 |
| No. of independent reflections | 6199 | 5246 | 1739 |
| No. of observed reflections | 4810 | 3471 | 1026 |
| Criterion for observed reflections | $F > 3\sigma(F)$ | $F > 3\sigma(F)$ | $F > 3\sigma(F)$ |
| $R_{int}$ | 0.024 | 0.0094 | 0.022 |
| $\theta_{max}$ (°) | 55 | 52.5 | 45 |
| Range of $h$, $k$, $l$ | $0 \rightarrow h \rightarrow 8$<br>$0 \rightarrow k \rightarrow 35$<br>$-21 \rightarrow l \rightarrow 21$ | $0 \rightarrow h \rightarrow 8$<br>$0 \rightarrow k \rightarrow 33$<br>$-21 \rightarrow l \rightarrow 20$ | $0 \rightarrow h \rightarrow 5$<br>$0 \rightarrow k \rightarrow 17$<br>$-10 \rightarrow l \rightarrow 10$ |
| No. of standard reflections | 3 | 3 | 1 |
| Frequency of standard reflections | Every 150 reflections | Every 150 reflections | Every 200 reflections |
| Intensity decay (%) | 8 | 5 | 1.5 |
| Refinement | | | |
| Refinement on | $F$ | $F$ | $F$ |
| $R$ | 0.054 | 0.057 | 0.060 |
| $wR$ | 0.056 | 0.066 | 0.068 |
| $S$ | 0.29 | 0.40 | — |
| No. of reflections used in refinement | 4810 | 3471 | 1026 |
| No. of parameters used | 106 | 106 | 137 |
| H-atom treatment | Only coordinates of H atoms refined | Only coordinates of H atoms refined | All H-atom parameters refined |
| Weighting scheme | $w = 1/[\sigma^2(F) + 0.08F^2]$ | $w = 1/[\sigma^2(F) + 0.08F^2]$ | $w = 1/[\sigma^2(F) + 0.04F^2]$ |
| $(\Delta/\sigma)_{max}$ | 0.01 | 0.01 | 0.01 |
| $\Delta\rho_{max}$ (e Å$^{-3}$) | 0.466 | 0.490 | — |
| $\Delta\rho_{min}$ (e Å$^{-3}$) | −0.258 | −0.182 | — |
| Extinction method | None | None | Isotropic (Zachariasen, 1967) |
| Source of atomic scattering factors | *International Tables for X-ray Crystallography* (1974, Vol. IV, Table 2.2B) | *International Tables for X-ray Crystallography* (1974, Vol. IV, Table 2.2B) | *International Tables for Crystallography* (1992, Vol. C) |
| Computer programs | | | |
| Data collection | Rigaku AFC-5 software | Rigaku AFC-5 software | 4-CND software |
| Cell refinement | *MSC/AFC Diffractometer Control Software* (Molecular Structure Corporation, 1988) | *MSC/AFC Diffractometer Control Software* (Molecular Structure Corporation, 1988) | *MSC/AFC Diffractometer Control Software* (Molecular Structure Coporation, 1988) |

Table 1 (*cont.*)

| | 150 K (X-ray) | 295 K (X-ray) | 295 K (neutron) |
|---|---|---|---|
| Data reduction | *MSC/AFC Diffractometer Control Software* (Molecular Structure Corporation, 1988) | *MSC/AFC Diffractometer Control Software* (Molecular Structure Corporation, 1988) | 4-CND software |
| Structure solution | *MULTAN*88 (Main *et al.*, 1988) | *MULTAN*88 (Main *et al.*, 1988) | *MULTAN*88 (Main *et al.*, 1988) |
| Structure refinement | Full-matrix least squares (Busing *et al.*, 1962) | Full-matrix least squares (Busing *et al.*, 1962) | Full-matrix least squares (Busing *et al.*, 1962) |

(4-CND) at Kyoto University Research Reactor Institute. The intensity measurements were carried out by the $\omega$-step-scan technique within $\sin\theta/\lambda = 0.762$ Å$^{-1}$. The crystal setting parameters were determined using the X-ray unit-cell parameters at 295 K. The coordinates and anisotropic displacement parameters of all atoms were refined by the full-matrix least-squares method. The scattering lengths used for C, O, N and H were 6.646, 5.803, 9.360 and $-3.741 \times 10^{-13}$ cm, respectively. Further details are given in Table 1.

### 2.3. *Electron density distribution*

The electron density distribution at 150 K was obtained using the modified maximum entropy method (Collins, 1982; Bricogne, 1984; Sato, 1992). The entropy (Shannon, 1949; Jaynes, 1957) for an electron density distribution is given by

$$S = -(V/N)\sum_{\mathbf{x}} \rho_{\mathbf{x}} \ln(\rho_{\mathbf{x}}/e),$$

where $V$ and $N$ denote the unit-cell volume and the number of equally divided pixels, respectively, and $\rho_{\mathbf{x}}$ is the average electron density in the pixel located at $\mathbf{x}$. The objective function $H$ was iteratively minimized with respect to $\rho_{\mathbf{x}}$ and Lagrange multipliers $\lambda_{\mathbf{h}}$ to obtain large $S$ and a small $R$ factor, using the sufficiently large positive constant $\omega$ ($\omega = 1.0$) according to

$$H = -S - \sum_{\mathbf{h}} \lambda_{\mathbf{h}} g_{\mathbf{h}} + (\omega/2)\sum_{\mathbf{h}} g_{\mathbf{h}}^2$$

where

$$g_{\mathbf{h}} = (|F_{\mathbf{h}}| - |F_{\mathbf{h}}^{\rm obs}|)/\sigma_{\mathbf{h}}.$$

The structure factors $F_{\mathbf{h}}$ were calculated by the direct Fourier transform of the electron density distribution in a unit cell and $\sigma_{\mathbf{h}}$ is the experimental standard uncertainty of the observed structure factors $F_{\mathbf{h}}^{\rm obs}$. The unit cell was divided into $32 \times 128 \times 64$ pixels and the initial electron densities were given by the Fourier transform of the observed structure factors with the phases from the last cycle of the usual least-squares refinement. During the course of the calculation, both the $R$ factor and entropy $S$ increased rapidly at first, then the $R$ factor decreased gradually without a significant decrease in $S$ after passing over the maximum values. The iteration was terminated when the $R$ factor reached a constant value and the $S$ value started to decrease again.

The electrostatic potential in the crystal was calculated from the charge density distribution using the Fourier-convolution-theorem method (Bertaut, 1978; Schwarzenbach & Thong, 1979). The charge distribution included point charges of the nucleus in addition to the electron charge distribution obtained by the maximum entropy method. The C, N and O nuclei were fixed at the positions of the least-squares refinement using X-ray data at low temperature, and the H atoms were located by referring to the results of the neutron diffraction study. The electron density distribution by the maximum entropy method was determined independently of the nuclei positions and the distribution was optimized within the experimental error of the observed structure factors. The subtle features in the electrostatic potential were calculated from these nuclei positions and this electron density distribution.

The crystallographic calculations were carried out using the program *KPPXRAY* (Taga *et al.*, 1991), including a modified version of *ORFLS* (Busing *et al.*, 1962) at the Data Processing Center, Kyoto University. The computer programs for the maximum entropy method and the calculation of the electrostatic potential were written in C language and the calculations were carried out on an HP712/60 workstation. The electron density maps and electrostatic maps were drawn using the program *XD2D* from the *XD* program package (Koritsanszky *et al.*, 1995).

## 3. Results and discussion

The final atomic coordinates and displacement parameters determined from the X-ray data at 150 K are listed in Table 2.† Bond lengths and angles are listed in Table 3. Fig. 1 shows the molecular structure with the atomic numbering scheme, and Fig. 2 shows a packing diagram viewed along the *a* axis.

The crystal structure is essentially the same as that obtained by Wright & King (1954). The bond lengths and angles obtained from the X-ray diffraction data at 295 K agree well with the results of Wright & King (1954), but the present parameters have been determined with one-order higher accuracy. The deviations of

† Supplementary data for this paper are available from the IUCr electronic archives (Reference: OA0014). Services for accessing these data are described at the back of the journal.

Table 2. *Fractional atomic coordinates and equivalent isotropic displacement parameters (Å²) from the X-ray data collected at 150 K*

$$U_{eq} = (1/3)\Sigma_i\Sigma_j U^{ij} a^i a^j \mathbf{a}_i.\mathbf{a}_j.$$

| | $x$ | $y$ | $z$ | $U_{eq}$ |
|---|---|---|---|---|
| C2 | −0.0384 (2) | 0.33937 (4) | 0.19344 (6) | 0.01989 (8) |
| C3 | 0.1528 (1) | 0.35815 (4) | 0.32749 (5) | 0.01734 (8) |
| C4 | 0.1745 (2) | 0.44285 (4) | 0.37152 (6) | 0.0231 (1) |
| C5 | 0.0184 (2) | 0.50592 (4) | 0.28065 (7) | 0.0265 (2) |
| C6 | −0.1644 (2) | 0.48110 (4) | 0.14914 (7) | 0.0235 (2) |
| C7 | 0.3283 (2) | 0.29179 (4) | 0.42823 (5) | 0.01934 (8) |
| N1 | −0.1976 (1) | 0.39949 (3) | 0.10545 (5) | 0.02188 (8) |
| N2 | 0.4058 (2) | 0.21699 (4) | 0.37214 (6) | 0.0240 (1) |
| O1 | 0.3963 (1) | 0.30857 (3) | 0.55835 (4) | 0.0272 (1) |

the constituent atoms of the pyridine ring from the least-squares best plane are less than 0.012 Å and the ring is planar within experimental error. The planar carboxamide group is rotated out of the plane of the pyridine ring. The O atom of the carboxamide group is in the proximity of the C4 atom of the pyridine ring; it is in the opposite direction to that observed in the indole-3-acetic acid/nicotinamide complex (Inoue *et al.*, 1978). The dihedral angle between the planes of the pyridine ring and the carboxamide group is 22.39 (4)° at 295 K and 22.16 (4)° at 150 K. The carboxamide orientation is similar to that observed in *N*-methylnicotinamide (Srikrishnan & Parthasarathy, 1990). The crystal structure consists of molecules stacking along the *a* axis and the planar pyridine rings are in contact with a plane-to-plane distance of 3.579 Å at 295 K and 3.475 Å at 150 K. Two intermolecular hydrogen bonds, N2···O1($x, \frac{1}{2}-y, -\frac{1}{2}+z$) and N2···N1($1+x, \frac{1}{2}-y, \frac{1}{2}+z$), are formed in the crystal. The hydrogen-bond parameters at room temperature are N···O 2.991 (1), H···O 2.101 (10) Å, N—H···O 175.3 (9)°, and N···N 3.105 (2), H···N 2.236 (10) Å, N—H···N 163.5 (9)°. As shown in the electrostatic potential map around the N2 atom in the $NH_2$ plane (Fig. 3), the positive peak around each H atom elongates toward the acceptor atoms. Since the positive potential field represents an electrophilic

Table 3. *Selected bond lengths (Å) and angles (°)*

| | X-ray diffraction | | Neutron diffraction |
|---|---|---|---|
| | 150 K | 295 K | 295 K |
| C2—C3 | 1.393 (1) | 1.390 (1) | 1.384 (1) |
| C2—N1 | 1.338 (1) | 1.337 (1) | 1.341 (1) |
| C3—C4 | 1.383 (1) | 1.379 (1) | 1.388 (1) |
| C3—C7 | 1.496 (1) | 1.498 (1) | 1.492 (1) |
| C4—C5 | 1.381 (1) | 1.376 (1) | 1.385 (1) |
| C5—C6 | 1.384 (1) | 1.375 (2) | 1.383 (1) |
| C6—N1 | 1.338 (1) | 1.332 (1) | 1.338 (1) |
| C7—N2 | 1.332 (1) | 1.329 (1) | 1.337 (1) |
| C7—O1 | 1.238 (1) | 1.234 (1) | 1.230 (1) |
| | | | |
| C2—HC2 | 0.928 (9) | 0.93 (1) | 1.074 (2) |
| C4—HC4 | 1.037 (9) | 1.02 (1) | 1.092 (2) |
| C5—HC5 | 0.93 (1) | 0.93 (1) | 1.082 (3) |
| C6—HC6 | 0.98 (1) | 1.00 (1) | 1.077 (2) |
| N2—HN2*A* | 0.88 (1) | 0.89 (1) | 1.000 (2) |
| N2—HN2*B* | 0.91 (1) | 0.89 (1) | 1.015 (2) |
| | | | |
| C3—C2—N1 | 123.01 (7) | 123.25 (8) | 123.10 (8) |
| C2—C3—C4 | 118.10 (5) | 117.73 (7) | 118.03 (9) |
| C2—C3—C7 | 123.81 (7) | 123.76 (8) | 124.08 (8) |
| C4—C3—C7 | 118.07 (7) | 118.49 (7) | 117.87 (9) |
| C3—C4—C5 | 119.62 (7) | 119.75 (8) | 119.52 (10) |
| C4—C5—C6 | 118.08 (8) | 118.22 (9) | 118.27 (9) |
| C5—C6—N1 | 123.55 (6) | 123.69 (8) | 123.10 (9) |
| C3—C7—N2 | 117.70 (6) | 117.92 (6) | 117.81 (8) |
| C3—C7—O1 | 119.16 (7) | 119.13 (8) | 119.72 (10) |
| N2—C7—O1 | 123.13 (6) | 122.96 (7) | 122.46 (11) |
| C2—N1—C6 | 117.59 (7) | 117.31 (7) | 117.95 (9) |
| | | | |
| C3—C2—HC2 | 124.3 (6) | 119.1 (6) | 121.51 (19) |
| N1—C2—HC2 | 112.5 (6) | 117.3 (6) | 115.36 (18) |
| C3—C4—HC4 | 116.6 (6) | 117.9 (7) | 118.45 (21) |
| C5—C4—HC4 | 123.8 (6) | 122.4 (7) | 122.01 (24) |
| C4—C5—HC5 | 118.6 (6) | 121.2 (6) | 121.48 (25) |
| C6—C5—HC5 | 123.1 (6) | 120.6 (6) | 120.24 (25) |
| C5—C6—HC6 | 121.9 (6) | 123.9 (7) | 120.36 (24) |
| N1—C6—HC6 | 114.5 (6) | 112.3 (6) | 116.54 (21) |
| C7—N2—HN2*A* | 121.6 (7) | 120.1 (7) | 121.25 (21) |
| C7—N2—HN2*B* | 117.2 (6) | 122.5 (6) | 118.45 (21) |

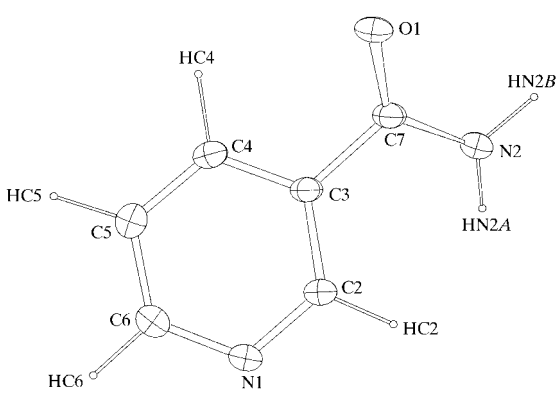


Fig. 1. The molecular structure with the atomic numbering scheme.

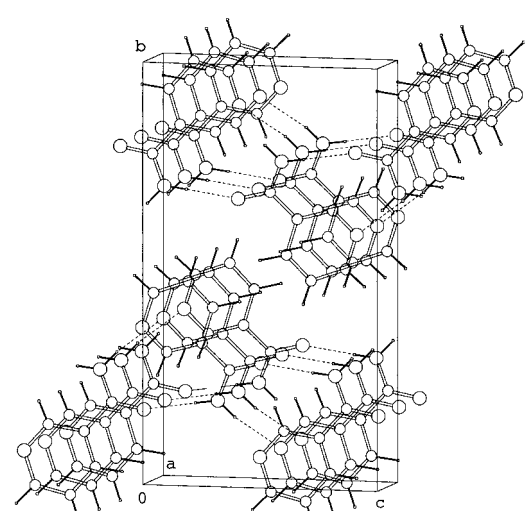


Fig. 2. A packing diagram viewed down the *a* axis.

area, the potential aspects observed here correspond to those of the preferable hydrogen bonds, although the hydrogen-bonding $NH_2$ plane twists by 12.6° with respect to the C3—C7—O1 plane and the O1 atom disappears from this map. No other intermolecular distances between non-H atoms are shorter than 3.2 Å. The crystal structure is held by these intermolecular hydrogen bonds and van der Waals forces.

The crystal lattice at low temperature shrinks significantly along the *a* axis in the stacking direction of the pyridine ring compared with that at high temperature (Table 1). The bond lengths at 150 K are, however, longer than those at 295 K, except for the C3—C7 single bond (Table 3). The shortening of the bond lengths could be attributed to the effects of large thermal motion at high temperature. Systematic differences are not found between the bond angles obtained from the X-ray data at 295 and 150 K. The skeletal bond lengths obtained from the neutron diffraction data at 295 K are longer than those from the X-ray data at the same temperature, except for C2—C3, C3—C7 and C7—O1. The bond lengths from the neutron diffraction study, if anything, are similar to the X-ray results at low temperature.

Fig. 4 shows the difference map between the observed electron density at 150 K and the calculated electron density assuming spherical atoms and their anisotropic displacement factors. The bonding density peaks of the covalent bonds in the molecule and a lone-pair density peak around N1 are clearly revealed and these peaks are comparable with those in other N-heteroaromatic rings (Wei *et al.*, 1994; Cunane & Taylor, 1993). The electrons in the pyridine ring localize near the carboxamide group, *i.e.* the bonding density peaks at the C3—C2 and C3—C4 bonds (0.30 and 0.35 e $Å^{-3}$) are higher than those at the C5—C4 and C5—C6 bonds (0.20 and 0.25 e $Å^{-3}$).

The electrostatic potential maps on three planes parallel to the pyridine ring are shown in Fig. 5. Figs. 5(*a*) and 5(*c*) show the electrostatic field maps at a distance of 0.874 Å above and below the pyridine-ring plane (Fig. 5*b*). The two maps are quite different to each other and they show asymmetry of the potential with respect to the pyridine-ring plane. The asymmetry is related to the twisting of the carboxamide group. The positive potential region near the C4 atom extends to the C═O-group side (Fig. 5*a*), while the positive potential regions near C2, HC2 and C6 extend somewhat to the $NH_2$-group side (Fig. 5*c*). The positive potential on C4 on the C═O side is larger than those of the other positive regions mentioned above and the opposite $NH_2$-group side of C4 (Fig. 5*c*) has a negative potential region. Such asymmetry of the potential on the C4 atom would facilitate hydride transfer from the side near the carbonyl group. This stereospecific property derived from the present study is consistent with the experimental and theoretical results studied so far (Donkersloot & Buck, 1981; de Kok *et al.*, 1986; Ohno *et al.*, 1986; Wu & Houk, 1991, 1993). Donkersloot & Buck (1981) pointed out that the stereospecificity is due to the interaction between the negatively charged O atom of the amide group and the positive charge of the donating moiety. The present result indicates that the stereospecificity of the $NAD^+$/NADH hydride-transfer reaction originates from the breaking of the symmetry of the electrostatic features on the C4 atom mainly induced by the oriented carboxamide group, in addition to the interaction of the amide oxygen with the hydride-donating group.

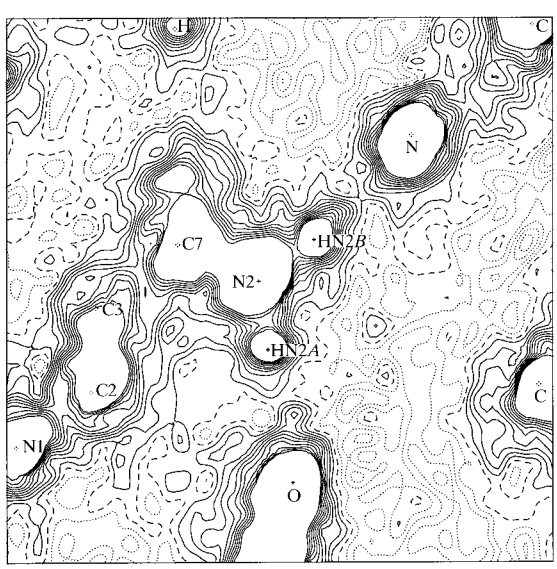


Fig. 3. The electrostatic potential map around the N2 atom in the $NH_2$ plane.

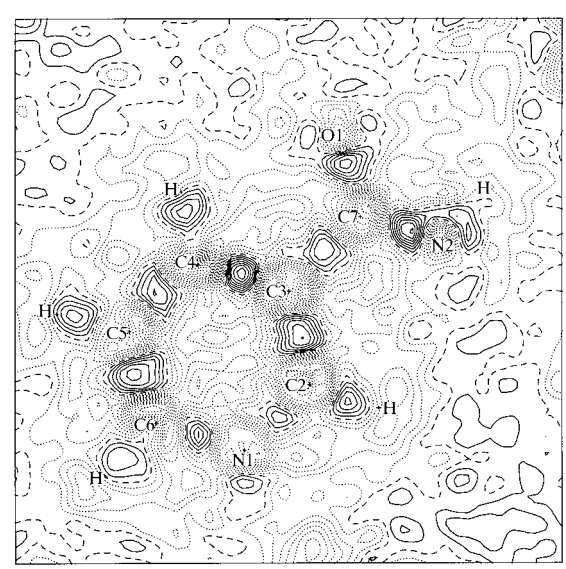


Fig. 4. The difference map in the plane of the pyridine ring. Contours are at 0.05 e $Å^{-3}$ intervals.

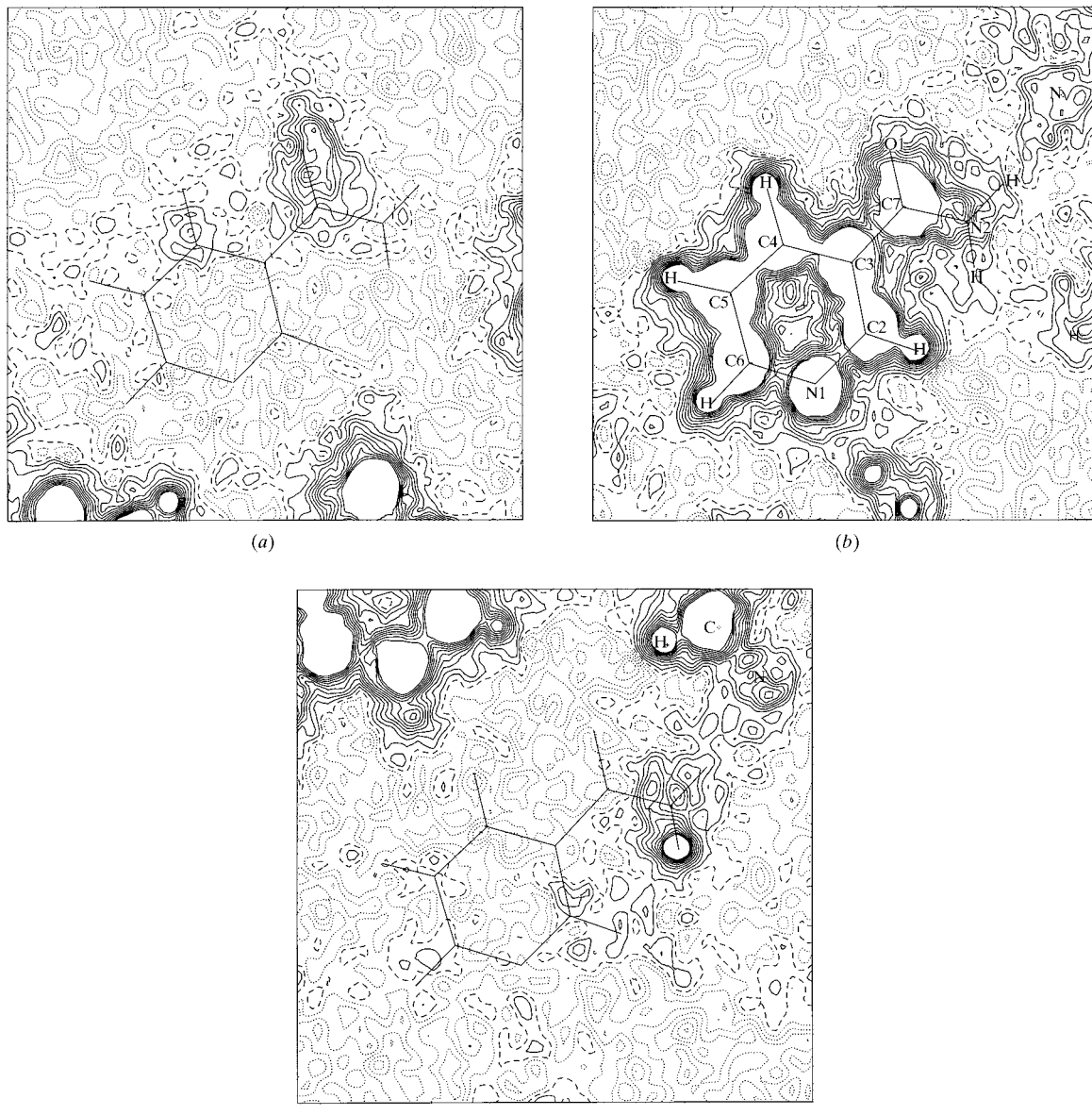


Fig. 5. The electrostatic potential maps in the planes parallel to the pyridine ring: (*a*) 0.874 Å above, (*b*) in and (*c*) 0.874 Å below the ring plane. Contours are at 0.5 e $Å^{-1}$ intervals.

## References


Bertaut, E. F. (1978). *J. Phys. Chem. Solids*, **39**, 97–102.

Bricogne, G. (1984). *Acta Cryst.* A**40**, 410–445.

Busing, W. R., Martin, K. O. & Levy, H. A. (1962). *ORFLS. Fortran Crystallographic Function and Error Program*. Report ORNL-TM-305. Oak Ridge National Laboratory, Tennessee, USA.

Collins, D. M. (1982). *Nature (London)*, **298**, 49–51.

Cunane, L. M. & Taylor, M. R. (1993). *Acta Cryst.* B**49**, 524–530.

Donkersloot, M. C. A. & Buck, H. M. (1981). *J. Am. Chem. Soc.* **103**, 6554–6558.

Inoue, M., Sakaki, T., Fujiwara, T. & Tomita, K. (1978). *Bull. Chem. Soc. Jpn*, **51**, 1118–1122.

Jaynes, E. T. (1957). *Phys. Rev.* **106**, 620–630.

Kok, P. M. T. de, Donkersloot, M. C. A., Van Lier, P. M., Meulendijks, G. H. W. M., Bastiaansen, L. A. M., Van Hooff, H. J. G., Kanters, J. A. & Buck, H. M. (1986). *Tetrahedron*, **42**, 941–959.

Koritsanszky, T., Howard, S., Mallinson, P. R., Su, Z., Richter, T. & Hansen, N. K. (1995). *XD. A Computer Program Package for Multipole Refinement and Analysis of Electron Densities from Diffraction Data*. Freie University Berlin, Germany, University of Wales Cardiff, Wales, University of Glasgow, Scotland, State University of New York at Buffalo, USA, and Université Henri Poincare, Nancy I, France.

Main, P., Hull, S. E., Lessinger, L., Germain, G., Declercq, J.-P. & Woolfson, M. M. (1988). *MULTAN88. A System of Computer Programs for the Automatic Solution of Crystal Structures from X-ray Diffraction Data*. Universities of York, England, and Louvain, Belgium.

Molecular Structure Corporation (1988). *MSC/AFC Diffractometer Control Software*. MSC, 3200 Research Forest Drive, The Woodlands, TX 77381, USA.

Nambiar, P. K., Stauffer, D. M., Kolodziej, P. A. & Benner, S. A. (1983). *J. Am. Chem. Soc.* **105**, 5886–5890.

Ohno, A., Kashiwagi, M. & Ishihara, Y. (1986). *Tetrahedron*, **42**, 961–973.

Sato, T. (1992). *Acta Cryst.* A**48**, 842–850.

Schwarzenbach, D. & Thong, N. (1979). *Acta Cryst.* A**35**, 652–658.

Shannon, C. E. (1949). *Proc. Inst. Radio Eng. NY*, **37**, 10–21.

Srikrishnan, T. & Parthasarathy, R. (1990). *Acta Cryst.* C**46**, 1723–1725.

Taga, T., Masuda, K., Higashi, T. & Iizuka, H. (1991). *KPPXRAY. Kyoto Program Package for X-ray Crystal Structure Analysis*. Kyoto University, Kyoto, Japan.

Wei, Y., Barton, R. & Robertson, B. (1994). *Acta Cryst.* B**50**, 161–174.

Wright, W. B. & King, G. S. D. (1954). *Acta Cryst.* **7**, 283–288.

Wu, Y.-D. & Houk, K. N. (1991). *J. Am. Chem. Soc.* **113**, 2353–2358.

Wu, Y.-D. & Houk, K. N. (1993). *J. Org. Chem.* **58**, 2043–2045.

You, K.-S., Arnold, L. J. Jr, Allison, W. S. & Kaplan, N. D. (1978). *Trends Biochem. Sci.* **3**, 265–268.

Zachariasen, W. H. (1967). *Acta Cryst.* **23**, 558–564.